



A. S. Kuleshov · E. S. Shalimova · A. Steindl

# On Hopf bifurcation in the problem of motion of a heavy particle on a rotating sphere: the viscous friction case

Received: 2 April 2019 / Revised: 18 September 2019 / Published online: 22 October 2019  
© The Author(s) 2019

**Abstract** We investigate the Hopf bifurcation of a mass on a rotating sphere under the influence of gravity and viscous friction. After determining the equilibria, we study their stability and calculate the first Lyapunov coefficient to determine the post-critical behavior. It is found that the bifurcating periodic branches are initially stable. For several inclination angles of the sphere's rotation axis, the periodic solutions are calculated numerically, which shows that for large inclination angles turning points occur, at which the periodic solutions become unstable. We also investigate the limiting case of small friction coefficients, when the mass moves close to the equator of the rotating sphere.

## 1 Introduction

The motion of bodies on surfaces is a classical problem of mechanics [1,2] and was investigated in various statements (see, for example, [3–6]). In the most simple case, a point particle instead of a rigid body could be considered. That kind of problems appears when we study the dynamics of mechanical systems with rotating parts performing different operations such as the mixing, grinding, and drying, of diverse substances. Based on results of computer simulations [7,8], it is possible to investigate the dynamics of systems with a large number of particles. However, the output of such a simulation usually does not represent any analytical results. That is why it is reasonable to consider simple systems, such as a particle moving on a surface under the action of a friction force. Even in these simple cases, some complex dynamic effects can be discovered. If there is a friction force and the surface doesn't move, the system will come to rest. However, if we assume that the surface rotates with a constant angular velocity, steady and periodic motions can appear in the system. This fact also makes it possible to use such problems to identify the friction coefficient. The problem of the motion of a point particle on a rotating surface was studied in [9]. The motion of a particle on a rotating table was investigated analytically and numerically in [10].

The problem of motion of a heavy bead on a circular hoop rotating about its vertical diameter has been studied in [11]. The similar problem for a circular hoop rotating about some other vertical axis has also been investigated [12]. In the present paper, a three-dimensional analogue of this problem is studied under the assumption that there is viscous friction between the point and the sphere.

---

A. S. Kuleshov · E. S. Shalimova  
Lomonosov Moscow State University, Moscow, Russia  
E-mail: kuleshov@mech.math.msu.su

E. S. Shalimova  
E-mail: ekaterina-shalimova@yandex.ru

A. Steindl (✉)  
Institute for Mechanics and Mechatronics, Technische Universität Wien, Vienna, Austria  
E-mail: Alois.Steindl@tuwien.ac.at

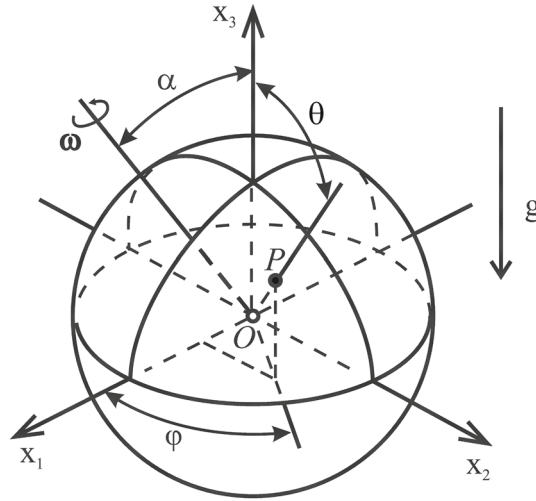


Fig. 1 A particle on a rotating sphere

**2 Definition of the problem and equations of motion**

Let  $P$  be a heavy particle of mass  $m$  which moves on a two-dimensional sphere of radius  $\ell$  under the action of a viscous friction force, with the coefficient of friction being  $c$ . The sphere rotates with a constant angular velocity  $\omega$  about a fixed axis. It is assumed that the axis passes through the center of the sphere  $O$ .

Let  $Ox_1x_2x_3$  be an absolute coordinate system such that the plane  $Ox_1x_2$  is horizontal and the axis  $e_3 = Ox_3$  is directed along the upward vertical, so the gravity force acting on the particle is  $-mge_3$ . Assume that the rotation axis belongs to the plane  $Ox_1x_3$  and its angle of inclination is  $\alpha$ ,  $0 \leq \alpha \leq \pi/2$ . Denote the spherical angles, which specify the position of the moving particle on the sphere, by  $\theta$  and  $\varphi$ ,  $0 \leq \theta \leq \pi$ ,  $0 \leq \varphi < 2\pi$  (Fig. 1).

In this case, the motion of the particle  $P$  can be described by the following system [15]:

$$\dot{\theta} = \gamma, \tag{1a}$$

$$\dot{\varphi} = \kappa, \tag{1b}$$

$$\dot{\gamma} = \sin \theta \cos \theta \kappa^2 + p \kappa \sin \theta - \chi \gamma - \chi \sin \alpha \sin \varphi, \tag{1c}$$

$$\dot{\kappa} = \frac{1}{\sin \theta} (\chi \sin \theta \cos \alpha - \chi \kappa \sin \theta - \chi \sin \alpha \cos \theta \cos \varphi - 2\gamma \kappa \cos \theta), \tag{1d}$$

where

$$p = \frac{mg}{c\ell\omega}, \quad \chi = \frac{c}{m\omega}.$$

System (1) possesses a symmetry w.r.t. mirror reflection about the  $(x_1, x_3)$ -plane: Inserting

$$\begin{aligned} \tilde{\theta} &= -\theta, & \tilde{\gamma} &= -\gamma, \\ \tilde{\varphi} &= \pi - \varphi, & \tilde{\kappa} &= -\kappa \end{aligned}$$

into (1), we obtain the same system of differential equations in the new variables.

**3 Equilibria positions and their stability**

Assuming  $\dot{\theta} = 0, \dot{\varphi} = 0, \dot{\gamma} = 0, \dot{\kappa} = 0$  we obtain the equations that determine the equilibria of the system:

$$0 = p \sin \theta_0 - \sin \alpha \sin \varphi_0, \tag{2a}$$

$$0 = \sin \theta_0 \cos \alpha - \sin \alpha \cos \theta_0 \cos \varphi_0. \tag{2b}$$

The system (2) can be solved for  $(\theta_0, \varphi_0)$  by introducing the quantities

$$u = \tan \theta_0, \quad v = \tan \varphi_0, \quad \text{with } \sin \theta_0 = \frac{u}{\sqrt{1+u^2}} \quad \text{and } \cos \theta_0 = \frac{1}{\sqrt{1+u^2}}.$$

Then (2b) gives

$$u = \frac{1}{\sqrt{1+v^2}} \tan \alpha,$$

which can be inserted in (2a):

$$p = \sin \alpha \frac{v}{\sqrt{1+v^2}} \frac{\sqrt{1+u^2}}{u} = \cos \alpha v \sqrt{1 + \frac{\tan^2 \alpha}{1+v^2}}. \tag{3}$$

By squaring both sides in (3) and rearranging, we obtain the quadratic equation for  $v^2$

$$\frac{p^2}{\cos^2 \alpha} (1+v^2) = v^2 (1+v^2 + \tan^2 \alpha). \tag{4}$$

Since

$$\frac{v^2}{1+v^2} (1+v^2 + \tan^2 \alpha) = v^2 + \tan^2 \alpha \frac{v^2}{1+v^2} = \tan^2 \varphi_0 + \tan^2 \alpha \sin^2 \varphi_0$$

increases monotonically for  $v > 0$ , Eq. (4) has one positive solution for  $v^2$ , the second solution of the quadratic equation leads to complex-valued solutions of  $\varphi_0$  and  $\theta_0$ .

Every positive solution of the quadratic equation (4) corresponds to 4 real-valued solutions for  $\varphi_0$ :

$$\varphi_{0,12} = \pm \arctan v \quad \text{and } \varphi_{0,34} = \varphi_{0,12} + \pi. \tag{5}$$

The corresponding stationary value of  $\theta_0$  can then be calculated by rewriting (2) as follows:

$$\sin \theta_0 = \sin \alpha \sin \varphi_0 / p, \quad \tan \theta_0 = \tan \alpha \cos \varphi_0, \quad \cos \theta_0 = \cos \alpha \tan \varphi_0 / p. \tag{6}$$

Due to the mirror reflection symmetry mentioned above, only two of these four solution pairs need to be investigated further, the stability and bifurcation behavior of the other two steady states follows by applying the mirror reflection.

The parameter  $\chi$  is a bifurcation parameter for system (1). However, it is convenient to introduce a parameter  $\lambda = \frac{1}{\chi}$  instead of  $\chi$ . Let us assume now that

$$\theta = \theta_0 + \hat{\theta}, \quad \varphi = \varphi_0 + \hat{\varphi}, \quad \gamma = \hat{\gamma}, \quad x = \hat{x},$$

where  $\hat{\theta}$ ,  $\hat{\varphi}$ ,  $\hat{\gamma}$ , and  $\hat{x}$  are small perturbations of the equilibria. Using (6) to eliminate  $\varphi_0$ , we can write the series expansion of the perturbed system up to the cubic terms as follows:

$$\dot{\hat{\theta}} = \hat{\gamma}, \tag{7a}$$

$$\dot{\hat{\varphi}} = \hat{x}, \tag{7b}$$

$$\begin{aligned} \dot{\hat{\gamma}} = & \frac{p}{\lambda} \cos \theta_0 \hat{\theta} - \frac{\sin \theta_0 \cos \alpha}{\lambda \cos \theta_0} \hat{\varphi} - \frac{1}{\lambda} \hat{\gamma} - \frac{p \sin \theta_0}{2\lambda} \hat{\theta}^2 + \frac{p \sin \theta_0}{2\lambda} \hat{\varphi}^2 \\ & + \sin \theta_0 \cos \theta_0 \hat{x}^2 - \frac{p \cos \theta_0}{6\lambda} \hat{\theta}^3 + \frac{\sin \theta_0 \cos \alpha}{6\lambda \cos \theta_0} \hat{\varphi}^3 + (\cos^2 \theta_0 - \sin^2 \theta_0) \hat{\theta} \hat{x}^2, \end{aligned} \tag{7c}$$

$$\begin{aligned} \dot{\hat{x}} = & \frac{\cos \alpha}{\lambda \sin \theta_0 \cos \theta_0} \hat{\theta} + \frac{p \cos \theta_0}{\lambda} \hat{\varphi} - \frac{1}{\lambda} \hat{x} - \frac{\cos \alpha}{\lambda \sin^2 \theta_0} \hat{\theta}^2 - \frac{p}{\lambda \sin \theta_0} \hat{\theta} \hat{\varphi} \\ & + \frac{\cos \alpha}{2\lambda} \hat{\varphi}^2 - \frac{2 \cos \theta_0}{\sin \theta_0} \hat{\gamma} \hat{x} + \left( \frac{\cos \alpha}{3\lambda \sin \theta_0 \cos \theta_0} + \frac{\cos \alpha \cos \theta_0}{\lambda \sin^3 \theta_0} \right) \hat{\theta}^3 \end{aligned}$$

$$+ \frac{p \cos \theta_0}{\lambda \sin^2 \theta_0} \hat{\theta}^2 \hat{\varphi} - \frac{\cos \alpha}{2\lambda \sin \theta_0 \cos \theta_0} \hat{\theta} \hat{\varphi}^2 + \frac{2}{\sin^2 \theta_0} \hat{\theta} \hat{\gamma} \hat{\chi} - \frac{p \cos \theta_0}{6\lambda} \hat{\varphi}^3. \quad (7d)$$

The linear part of the system (7) is

$$\dot{\mathbf{x}} = \mathbf{F}(\lambda)\mathbf{x}, \quad (8)$$

where

$$\mathbf{x} = (\hat{\theta}, \hat{\varphi}, \hat{\gamma}, \hat{\chi})$$

and

$$\mathbf{F}(\lambda) = \begin{pmatrix} 0 & 0 & 1 & 0 \\ 0 & 0 & 0 & 1 \\ \frac{p}{\lambda} \cos \theta_0 & -\frac{\sin \theta_0 \cos \alpha}{\lambda \cos \theta_0} & -\frac{1}{\lambda} & 0 \\ \frac{\cos \alpha}{\lambda \sin \theta_0 \cos \theta_0} & \frac{p}{\lambda} \cos \theta_0 & 0 & -\frac{1}{\lambda} \end{pmatrix}.$$

The characteristic equation of the linearized system is

$$P(\sigma) = \det(\mathbf{F}(\lambda) - \sigma \mathbf{E}) = \sigma^4 + b_1 \sigma^3 + b_2 \sigma^2 + b_3 \sigma + b_4, \quad (9)$$

where

$$b_1 = \frac{2}{\lambda}, \quad b_2 = \frac{1 - 2\lambda p \cos \theta_0}{\lambda^2}, \quad b_3 = -\frac{2p \cos \theta_0}{\lambda^2}, \quad b_4 = \frac{p^2 \cos^2 \theta_0}{\lambda^2} + \frac{\cos^2 \alpha}{\lambda^2 \cos^2 \theta_0}.$$

The Routh–Hurwitz criterion leads to the following stability conditions:

$$b_1 > 0, \quad b_2 > 0, \quad b_3 > 0, \quad b_4 > 0, \quad R \equiv b_1 b_2 b_3 - b_4 b_1^2 - b_3^2 > 0. \quad (10)$$

Now we will consider the obtained conditions. Taking into account the form of the coefficient  $b_1$ , the first condition is equivalent to

$$\lambda > 0. \quad (11)$$

The third condition  $b_3 > 0$  is equivalent to

$$p \cos \theta_0 < 0. \quad (12)$$

Taking into account (11) and (12), the second and the fourth conditions are also satisfied. The last condition  $R > 0$  can be rewritten as follows:

$$R = -\frac{4(p \cos^3 \theta_0 + \lambda \cos^2 \alpha)}{\lambda^5 \cos^2 \theta_0} > 0.$$

This condition holds when

$$\lambda < \lambda_0 = -\frac{p \cos^3 \theta_0}{\cos^2 \alpha}.$$

Since  $b_4 = \det(F(\lambda)) > 0$  for  $p \neq 0$  and  $\cos \alpha \neq 0$ , there cannot occur a steady-state bifurcation. The boundary of a stability region is given by the condition  $R = 0$ . On this boundary the characteristic equation has a pair of purely imaginary roots. The type of the second pair of roots on the boundary depends on the sign of the expression

$$\Delta_1^* = \left( \frac{b_1 b_4}{b_3} - \frac{b_1^2}{4} \right)_{\lambda=\lambda_0} = \frac{\cos^2 \alpha}{\cos^2 \theta_0} > 0.$$

Thus, on the boundary  $R = 0$  the characteristic equation (9) has the roots

$$\sigma_1 = bi, \quad \sigma_2 = -bi, \quad \sigma_3 = m + ni, \quad \sigma_4 = m - ni,$$

where

$$b^2 = \left(\frac{b_3}{b_1}\right)_{\lambda=\lambda_0}, \quad m = -\left(\frac{b_1}{2}\right)_{\lambda=\lambda_0}, \quad n^2 = \left(\frac{b_1 b_4}{b_3} - \frac{b_1^2}{4}\right)_{\lambda=\lambda_0}, \quad n > 0.$$

As shown in [15], in this case

$$p > 0, \quad \cos \theta_0 < 0,$$

so

$$n = -\frac{\cos \alpha}{\cos \theta_0}, \quad b = n, \quad m = \frac{\cos^2 \alpha}{p \cos^3 \theta_0}.$$

Thus, the system has two purely imaginary roots and two roots with a negative real part. This fact allows us to suggest a branching of a limit cycle when  $\lambda = \lambda_0$ . Such a bifurcation was found numerically, and so it is also reasonable to study the bifurcation analytically.

The dependence of the system behavior near the stability boundary  $R = 0$  on the parameter  $\lambda$  is determined by theorems given below. Consider the variation of the parameter  $\lambda$  on a small interval  $\lambda_0 - \eta \leq \lambda \leq \lambda_0 + \eta$ , where  $\lambda_0$  can be found from  $R(\lambda_0) = 0$ . Let  $a = L_1(\lambda_0)$  be the first Lyapunov coefficient given below that determines the stability for  $\lambda = \lambda_0$ . Neglecting higher-order terms, the behavior of the system close to the bifurcation point can be described by the one-dimensional differential equation for the radius of the bifurcating periodic solution

$$\dot{r} = -d(\lambda - \lambda_0)r + ar^3, \tag{13}$$

where  $d = -d\sigma_c/d\lambda \propto dR/d\lambda$ , evaluated at the Hopf bifurcation point.

**Theorem 1** (Supercritical Hopf bifurcation [17]) *Let*

$$a = L_1(\lambda_0) < 0, \quad d = \frac{-d\sigma_c}{d\lambda}_{\lambda=\lambda_0} < 0,$$

*then (13) has a non-trivial asymptotically stable stationary solution  $r = (d(\lambda - \lambda_0)/a)^{1/2}$  for  $\lambda > \lambda_0$ .*

Thus, with increasing  $\lambda$ , the stable equilibrium becomes unstable, but the image point stays in an  $\varepsilon$ -neighborhood of the equilibrium. With decreasing  $\lambda$ , the equilibrium becomes stable again and the image point returns to the equilibrium, as shown in Fig. 2. The behavior of the system is reversible with respect to  $\lambda$ .

The proof of this theorem has been described in detail [13, 14, 16, 17].

**Theorem 2** (Subcritical Hopf bifurcation) *If  $a = L_1(\lambda_0) > 0$  and  $d = dR/d\lambda_{\lambda=\lambda_0} < 0$ , then (13) has a non-trivial asymptotically unstable stationary solution  $r = (d(\lambda - \lambda_0)/a)^{1/2}$  for  $\lambda < \lambda_0$ . For  $\lambda > \lambda_0$  the trivial solution is unstable and no nearby stable stationary solution exists.*

Thus, with increasing  $\lambda$  the stable equilibrium becomes unstable, and the point leaves the neighborhood of it. When  $\lambda$  is decreased again below  $\lambda_0$ , the point will usually not return to the equilibrium. The behavior of the system is therefore irreversible with respect to  $\lambda$ . A typical situation is shown in Fig. 3 for a locally subcritical, but globally supercritical Hopf bifurcation: If  $\lambda$  increases beyond the critical value  $\lambda_c$ , the system quickly moves to the stable large amplitude oscillation and remains there, even if  $\lambda$  decreases below  $\lambda_0$  again. Only if it reaches the limit point cycle (“LP”), it jumps back to the stationary state, exhibiting a hysteretic behavior.

This theorem has also been proved in [13].

In the case under consideration, we have

$$\left(\frac{dR}{d\lambda}\right)_{\lambda=\lambda_0} = \frac{4 \cos^{12} \alpha}{p^5 \cos^{17} \theta_0} < 0.$$

In this case, the first Lyapunov coefficient has the form (see the Appendix)

$$L_1(\lambda_0) = -\frac{\pi \cos^7 \alpha \sin^2 \theta_0}{p \cos^6 \theta_0 (4p^2 \cos^4 \theta_0 + \cos^2 \alpha)}. \tag{14}$$

Since  $\cos \alpha > 0$  and  $p > 0$ , this expression is negative. Therefore, the system satisfies the conditions of Theorem 1, and the boundary  $R = 0$  is safe. Periodic modes that appear when  $\lambda > \lambda_0$  are stable.

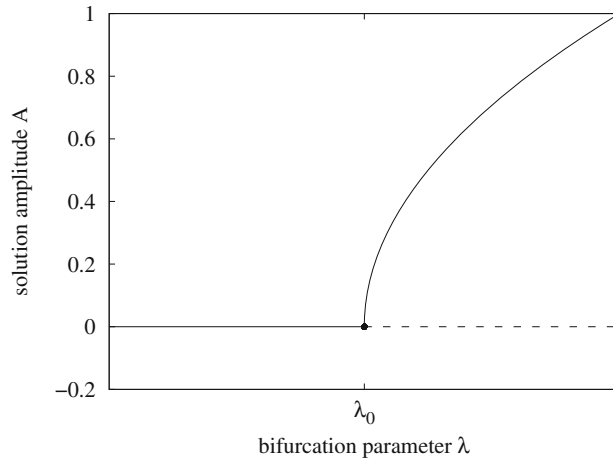


**Fig. 2** Bifurcation diagram for the supercritical Hopf bifurcation. When  $\lambda$  is increased beyond  $\lambda_0$ , the periodic solutions remain nearby the stationary state and return to the stationary solution, if  $\lambda$  is decreased below  $\lambda_0$

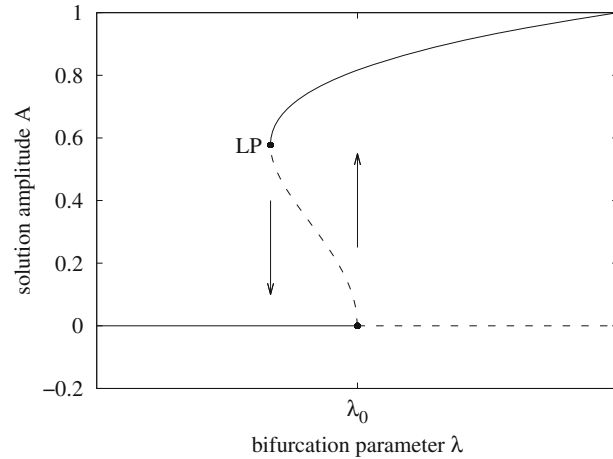


**Fig. 3** Bifurcation diagram for a globally supercritical, but locally subcritical Hopf bifurcation. If  $\lambda$  increases beyond  $\lambda_0$ , the system jumps up to the stable large periodic solution and remains there, even if  $\lambda$  becomes slightly smaller than  $\lambda_0$  again

**4 Numerical investigation of the bifurcating solutions**

Since by (14) the first Lyapunov equation  $L_1(\lambda_0)$  is negative for all parameter values, the bifurcating periodic solutions exist locally for  $\lambda \geq \lambda_0$ , respectively, for friction coefficients  $\chi \leq \chi_0 = 1/\lambda_0$ . In order to get the global behavior, several branches of periodic solutions were computed by the BVP solver Boundsco [18] and the continuation algorithm Hom [19] for fixed values of  $p = 3$  and inclination angle  $\alpha$  for varying values of the distinguished parameter  $\chi$ . As can be seen in Fig. 4, the periodic solutions are throughout stable for small inclination angles  $\alpha$  and extend down to  $\chi = 0$ . For inclination angles  $\alpha > \alpha_c \approx 54.8^\circ$ , the branches display turning points, where the stability of the periodic solutions changes. For values of  $\chi$  between the turning points, three different periodic solutions are found, two of these are stable and the medium one is unstable. For  $\alpha = 75^\circ$  and  $\chi = 0.02$ , the periodic solutions are displayed in Fig. 5. The largest orbit is almost aligned with the equator of the rotating sphere, whereas the smallest solution oscillates close to the bottom of the sphere.

During the path-following along the periodic solutions, we encounter a singularity of the differential equations due to the use of spherical coordinates: Close to the Hopf bifurcation point the solutions are periodic in  $\theta$  and  $\varphi$ ; but after the trajectories pass through the south pole of the sphere, the azimuthal angle  $\varphi$  increases by  $2\pi$  during one period. In order to overcome this difficulty, a different coordinate system (Cartesian or spherical coordinates along the rotation axis) has been used close to the crossing of the south pole, when the equations become singular.

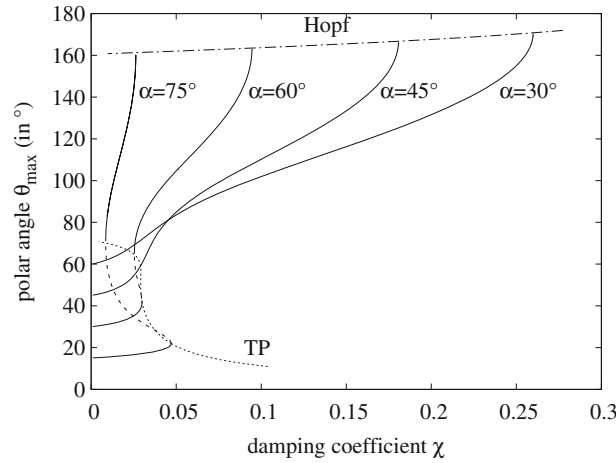


**Fig. 4** Bifurcation diagram for  $p = 3$  and different inclination angles  $\alpha$  in the  $(\chi, \theta)$ -plane. The periodic solutions bifurcate from the Hopf bifurcation boundary (“Hopf”). Stable (unstable) solutions are displayed as solid (dashed) lines, respectively. The curve “TP” shows the location of turning points for varying inclination angles  $\alpha$

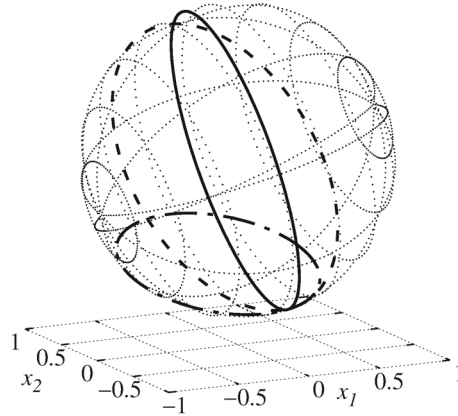


**Fig. 5** Periodic solutions for  $\alpha = 75^\circ$  and  $\chi = 0.02$ . The polar axis for the spherical coordinates is oriented along the rotation axis of the sphere (color figure online)

4.1 Limiting behavior for small friction coefficients

When the parameter  $\chi$  is set to zero, all gravitational and damping forces vanish and the mass can move freely on the sphere, tracing out arbitrary great circles. For small values of  $\chi$ , or equivalently, for large rotation speeds  $\omega$ , the numerical calculations indicate that the periodic solution approaches the equator of the rotating sphere and rotates with the same speed as the sphere. That behavior is also expected by mechanical reasoning: If we neglect the gravitational force, the friction and centrifugal force will cause the mass to move along the equator; a small gravitational force causes a periodic excitation.

In order to study this motion, we use spherical angles aligned with the rotation axis of the sphere. In these coordinates, the friction terms become simpler, by setting  $\alpha = 0$  in (1), because in the new coordinate system the sphere rotates about the  $z$ -axis. Since now the gravity acts in the direction  $\mathbf{e}_g = (\sin \alpha, 0, -\cos \alpha)^T$ , its potential becomes

$$V = -\chi p \mathbf{e}_g \cdot (\sin \theta \cos \varphi, \sin \theta \sin \varphi, \cos \theta)^T = \chi p (\cos \theta \cos \alpha - \sin \theta \cos \varphi \sin \alpha).$$

The equations of motion are therefore given by

$$\dot{\theta} = \gamma, \tag{15a}$$

$$\dot{\varphi} = \kappa, \tag{15b}$$

$$\dot{\gamma} = \sin \theta \cos \theta \kappa^2 + p \chi (\sin \theta \cos \alpha + \cos \theta \cos \varphi \sin \alpha) - \chi \gamma, \tag{15c}$$

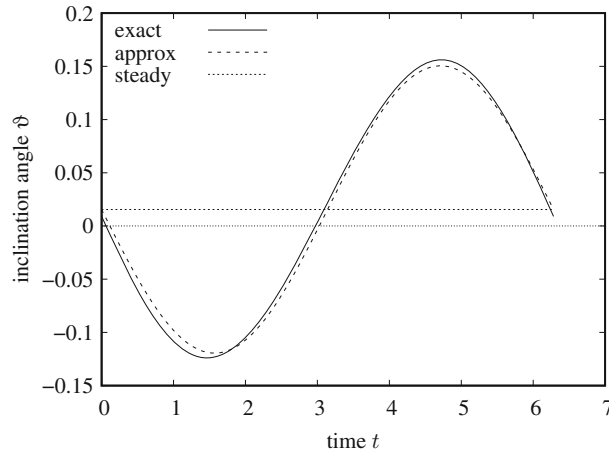


**Fig. 6** Numerical “exact” solution and approximation  $\vartheta = \vartheta_0 + \vartheta_1$  of (15a)–(15d) for the parameter values  $p = 3$ ,  $\chi = 0.02$ ,  $\alpha = 75^\circ$  corresponding to the periodic solutions displayed in Fig. 5. The numerical solution corresponds to the solid, steep curve in Fig. 5. The steady contribution  $\vartheta_0$  is displayed by the dotted line

$$\dot{\kappa} = \frac{1}{\sin \theta} (\chi \sin \theta (1 - \kappa) - p\chi \sin \theta \sin \varphi \sin \alpha - 2\gamma\kappa \cos \theta). \quad (15d)$$

For  $p = 0$  a solution of (15a)–(15d) is given by the steady rotation  $\theta = \pi/2$ ,  $\varphi = t$  along the equator. Since Eq. (15d) for  $\kappa$  is dominated by the term  $\chi(1 - \kappa)$ , the azimuthal dynamics will change slightly under the perturbation by  $p$ : At leading order, we obtain from (15d)

$$\dot{\varphi} = \kappa = 1 - \int^t p\chi \sin \tau \sin \alpha d\tau = 1 + p\chi \cos t \sin \alpha, \quad (16)$$

where the integration constant has been chosen such that the average perturbation of  $\kappa$  vanishes. Setting  $\theta = \pi/2 + \vartheta$ ,  $\kappa^2 \approx 1 + 2p\chi \cos t \sin \alpha$  and expanding Eq. (15c) up to first order in  $\chi$ , we obtain the linear equation with parametric excitation

$$\ddot{\vartheta} + \chi \dot{\vartheta} + (1 + 3p\chi \sin \alpha \cos t)\vartheta = p\chi \cos \alpha. \quad (17)$$

One might think that the leading order expansion

$$\vartheta_0 = p\chi \cos \alpha \quad (18)$$

yields a good approximation for small  $\chi$ , but the numerical solutions show a large periodic deviation from this estimate, which occurs, because the parametric excitation frequency in (17) is in 1 : 1 resonance with the eigenfrequency of the unperturbed equation. In order to find the periodic component of  $\vartheta$ , we set  $\vartheta = \vartheta_0 + \vartheta_1$  and obtain the differential equation

$$\ddot{\vartheta}_1 + \chi \dot{\vartheta}_1 + (1 + 3p\chi \sin \alpha \cos t)\vartheta_1 = -3p^2\chi^2 \sin \alpha \cos \alpha \cos t. \quad (19)$$

In order to find the influence of the parametric excitation term  $3p\chi \sin \alpha \sin t \vartheta_1$ , we apply two steps of Normal Form reduction to the equation to find the periodic solution

$$\vartheta_1 = 3p^2\chi \sin \alpha \cos \alpha \sin t, \quad (20)$$

which satisfies (19) up to terms of order  $O(\chi^2)$ .

As demonstrated in Fig. 6, this approximation agrees well with the numerically obtained periodic solution of the nonlinear equation, while the steady approximation is very poor.



### 5 Conclusions

The Hopf bifurcation of a moving mass on a rotating sphere has been investigated. By transforming the system to Jordan Normal Form, calculating the Center Manifold and simplifying the system using Normal Form theory we obtained a simple expression for the first Lyapunov coefficient. Since this coefficient is negative, the periodic solutions bifurcate supercritically from the steady state. These bifurcating solutions are also computed numerically, and their limiting behavior for vanishing friction force is studied.

**Acknowledgements** Open access funding provided by TU Wien (TUW).

**Open Access** This article is distributed under the terms of the Creative Commons Attribution 4.0 International License (<http://creativecommons.org/licenses/by/4.0/>), which permits unrestricted use, distribution, and reproduction in any medium, provided you give appropriate credit to the original author(s) and the source, provide a link to the Creative Commons license, and indicate if changes were made.

### A Calculation of the Lyapunov coefficient

For the case under consideration, a pair of eigenvalues  $\pm i\omega$  on the imaginary axis and a second complex conjugate pair  $m \pm in$  with  $m < 0$ , the Lyapunov coefficient was already derived in [13]. Since this formula looks extremely complicated, the contributions from the cubic terms in (24) from Normal Form calculations and from Center Manifold Reduction are stated separately.

#### A.1 Transformation to Jordan Normal Form

The first step to calculate the bifurcating solutions is to introduce a linear change of coordinates, which transforms the linearized equations (8) at the steady state to real Jordan Normal Form: Let  $v_c$  and  $v_s$  be the complex valued eigenvectors of the Jacobian  $F$  corresponding to the eigenvalues  $i\omega$  and  $m + in$ , respectively, then the matrix

$$V = [\Re(v_c), \Im(v_c), \Re(v_s), \Im(v_s)] \tag{21}$$

satisfies

$$FV = VJ \quad \text{with } J = \begin{pmatrix} 0 & -\omega & 0 & 0 \\ \omega & 0 & 0 & 0 \\ 0 & 0 & m & -n \\ 0 & 0 & n & m \end{pmatrix}.$$

Setting

$$x = J\xi \tag{22}$$

transforms system (7) to the new nonlinear system

$$\dot{\xi} = J\xi + f(\xi) \quad \text{with } f(\xi) = V^{-1}F_{NL}(V\xi), \tag{23}$$

where  $F_{NL}(x)$  contains the nonlinearities of (7). The explicit formulas for the entries of  $V$  and  $f(\xi)$  are given below.

In the transformed coordinates, the system takes the following form:

$$\dot{\xi}_1 = -b\xi_2 + Q_1(\xi_1, \xi_2, \xi_3, \xi_4), \tag{24a}$$

$$\dot{\xi}_2 = b\xi_1 + Q_2(\xi_1, \xi_2, \xi_3, \xi_4), \tag{24b}$$

$$\dot{\xi}_3 = m\xi_3 - n\xi_4 + Q_3(\xi_1, \xi_2, \xi_3, \xi_4), \tag{24c}$$

$$\dot{\xi}_4 = n\xi_3 + m\xi_4 + Q_4(\xi_1, \xi_2, \xi_3, \xi_4), \tag{24d}$$

where  $b, n, m$  are defined by the solutions of the characteristic equation (9).

The nonlinear part of Eq. (7) can be rewritten as:

$$\begin{aligned}
 P_v(x_1, x_2, x_3, x_4) = & a_{11}^{(v)} x_1^2 + a_{22}^{(v)} x_2^2 + a_{33}^{(v)} x_3^2 + a_{44}^{(v)} x_4^2 \\
 & + 2a_{12}^{(v)} x_1 x_2 + 2a_{13}^{(v)} x_1 x_3 + 2a_{14}^{(v)} x_1 x_4 + 2a_{23}^{(v)} x_2 x_3 + 2a_{24}^{(v)} x_2 x_4 + 2a_{34}^{(v)} x_3 x_4 \\
 & + a_{111}^{(v)} x_1^3 + a_{222}^{(v)} x_2^3 + a_{333}^{(v)} x_3^3 + a_{444}^{(v)} x_4^3 \\
 & + 3a_{112}^{(v)} x_1^2 x_2 + 3a_{113}^{(v)} x_1^2 x_3 + 3a_{114}^{(v)} x_1^2 x_4 + 3a_{221}^{(v)} x_2^2 x_1 + 3a_{223}^{(v)} x_2^2 x_3 + 3a_{224}^{(v)} x_2^2 x_4 \\
 & + 3a_{331}^{(v)} x_3^2 x_1 + 3a_{332}^{(v)} x_3^2 x_2 + 3a_{334}^{(v)} x_3^2 x_4 + 3a_{441}^{(v)} x_4^2 x_1 + 3a_{442}^{(v)} x_4^2 x_2 + 3a_{443}^{(v)} x_4^2 x_3 \\
 & + 6a_{123}^{(v)} x_1 x_2 x_3 + 6a_{124}^{(v)} x_1 x_2 x_4 + 6a_{134}^{(v)} x_1 x_3 x_4 + 6a_{234}^{(v)} x_2 x_3 x_4 + \dots,
 \end{aligned}$$

where

$$\begin{aligned}
 a_{11}^{(3)} &= -\frac{p \sin \theta_0}{2\lambda}, & a_{22}^{(3)} &= \frac{p \sin \theta_0}{2\lambda}, & a_{44}^{(3)} &= \sin \theta_0 \cos \theta_0, \\
 a_{111}^{(3)} &= -\frac{p \cos \theta_0}{6\lambda}, & a_{222}^{(3)} &= \frac{\sin \theta_0 \cos \alpha}{6\lambda \cos \theta_0}, & a_{441}^{(3)} &= \frac{(\cos^2 \theta_0 - \sin^2 \theta_0)}{3}, \\
 a_{11}^{(4)} &= -\frac{\cos \alpha}{\lambda \sin^2 \theta_0}, & a_{22}^{(4)} &= \frac{\cos \alpha}{2\lambda}, & a_{12}^{(4)} &= -\frac{p}{2\lambda \sin \theta_0}, \\
 a_{34}^{(4)} &= -\frac{\cos \theta_0}{\sin \theta_0}, & a_{111}^{(4)} &= \left( \frac{\cos \alpha}{3\lambda \sin \theta_0 \cos \theta_0} + \frac{\cos \alpha \cos \theta_0}{\lambda \sin^3 \theta_0} \right), & a_{222}^{(4)} &= -\frac{p \cos \theta_0}{6\lambda}, \\
 a_{112}^{(4)} &= \frac{p \cos \theta_0}{3\lambda \sin^2 \theta_0}, & a_{221}^{(4)} &= -\frac{\cos \alpha}{6\lambda \sin \theta_0 \cos \theta_0}, & a_{134}^{(4)} &= \frac{1}{6 \sin^2 \theta_0},
 \end{aligned}$$

and the other coefficients are zero. Then the corresponding coefficients of the nonlinear part of the transformed system are:

$$\begin{aligned}
 A_{11}^{(1)} &= -\frac{1}{2} \frac{\beta(2 \cos \theta_0 \beta^2 \lambda + \cos^2 \theta_0 p - 4\beta \cos \alpha \lambda - p)}{(4\beta^2 \lambda^2 + 1)\lambda}, \\
 A_{22}^{(1)} &= -\frac{1}{2} \frac{\beta(2\beta \cos \alpha \lambda + p)}{(4\beta^2 \lambda^2 + 1)\lambda}, & A_{12}^{(1)} &= \frac{\beta^2(2 \cos \theta_0 \beta^2 \lambda - p)}{4\beta^2 \lambda^2 + 1}, \\
 A_{13}^{(1)} &= \frac{1}{2} \frac{\beta^2(-2 \cos \theta_0 \beta^2 \lambda + \cos^2 \theta_0 p - p)}{(4\beta^2 \lambda^2 + 1)\lambda \sin \theta_0}, & A_{14}^{(1)} &= -\frac{\beta^3(2 \cos \theta_0 \beta^2 \lambda^2 + \lambda p + \cos \theta_0)}{(4\beta^2 \lambda^2 + 1)\lambda \sin \theta_0}, \\
 A_{23}^{(1)} &= \frac{\beta^3(2 \cos \theta_0 \beta^2 \lambda + p)}{(4\beta^2 \lambda^2 + 1) \sin \theta_0}, & A_{24}^{(1)} &= -\frac{1}{2} \frac{\beta^2(-4 \cos \theta_0 \beta^2 \lambda + 2 \cos \alpha \beta \lambda + p)}{(4\beta^2 \lambda^2 + 1)\lambda \sin \theta_0}, \\
 A_{11}^{(2)} &= -\frac{\beta(2 \cos \theta_0 \beta^3 \lambda^2 + \cos^2 \theta_0 \beta \lambda p + \cos \alpha - \beta \lambda p)}{(4\beta^2 \lambda^2 + 1)\lambda}, \\
 A_{22}^{(2)} &= \frac{1}{2} \frac{\beta(-2\beta \lambda p + \cos \alpha)}{(4\beta^2 \lambda^2 + 1)\lambda}, & A_{12}^{(2)} &= -\frac{1}{2} \frac{\beta(2 \cos \theta_0 \beta^2 \lambda - p)}{(4\beta^2 \lambda^2 + 1)\lambda}, \\
 A_{13}^{(2)} &= \frac{\beta^3(-2 \cos \theta_0 \beta^2 \lambda + \cos^2 \theta_0 p - p)}{(4\beta^2 \lambda^2 + 1) \sin \theta_0}, & A_{14}^{(2)} &= -\frac{1}{2} \frac{\beta^2(2 \cos \theta_0 \beta^2 \lambda - p)}{(4\beta^2 \lambda^2 + 1)\lambda \sin \theta_0}, \\
 A_{23}^{(2)} &= -\frac{1}{2} \frac{\beta^2(2 \cos \theta_0 \beta^2 \lambda + p)}{(4\beta^2 \lambda^2 + 1)\lambda \sin \theta_0}, & A_{24}^{(2)} &= \frac{1}{2} \frac{\beta^2(-2\beta \lambda p - 2 \cos \theta_0 \beta + \cos \alpha)}{(4\beta^2 \lambda^2 + 1)\lambda \sin \theta_0}, \\
 A_{11}^{(3)} &= \frac{1}{2} \frac{\sin \theta_0(-2 \cos \theta_0 \beta^2 \lambda - \cos^2 \theta_0 p + 4 \cos \alpha \beta \lambda + p)}{(4\beta^2 \lambda^2 + 1)\lambda}, \\
 A_{22}^{(3)} &= -\frac{1}{2} \frac{\sin \theta_0(2 \cos \alpha \beta \lambda + p)}{(4\beta^2 \lambda^2 + 1)\lambda}, & A_{12}^{(3)} &= \frac{\beta \sin \theta_0(2 \cos \theta_0 \beta^2 \lambda - p)}{4\beta^2 \lambda^2 + 1}, \\
 A_{11}^{(4)} &= \frac{\sin \theta_0(2 \cos \theta_0 \beta^3 \lambda^2 + \cos^2 \theta_0 \beta \lambda p - \beta \lambda p + \cos \alpha)}{(4\beta^2 \lambda^2 + 1)\lambda},
 \end{aligned}$$

$$A_{22}^{(4)} = -\frac{1 \sin \theta_0 (-2\beta\lambda p + \cos \alpha)}{2(4\beta^2\lambda^2 + 1)\lambda}, \quad A_{12}^{(4)} = \frac{1 \sin \theta_0 (2 \cos \theta_0 \beta^2 \lambda - p)}{2(4\beta^2\lambda^2 + 1)\lambda}.$$

with  $\beta = \cos \alpha / \cos \theta_0$ .

The first Lyapunov coefficient can be found as follows [13]:

$$L_1(\lambda_0) = \frac{\pi}{4b^2} \left( L_{1,\text{cub}} + L_{1,\text{nf}} + \frac{2b}{\Delta} L_{1,\text{cm}} \right) \tag{25}$$

with

$$\begin{aligned} L_{1,\text{cub}} &= 3b(A_{111}^{(1)} + A_{222}^{(2)} + A_{112}^{(2)} + A_{122}^{(1)}), \\ L_{1,\text{nf}} &= 2(A_{22}^{(1)}A_{22}^{(2)} - A_{11}^{(1)}A_{11}^{(2)}) - 2A_{12}^{(2)}(A_{11}^{(2)} + A_{22}^{(2)}) + 2A_{12}^{(1)}(A_{11}^{(1)} + A_{22}^{(1)}), \\ L_{1,\text{cm}} &= 2(A_{23}^{(1)} + A_{13}^{(2)})(m^2 + n^2)[b(n^2 - m^2 - 4b^2)A_{11}^{(3)} + m(n^2 + 4b^2 + m^2)A_{12}^{(3)} \\ &\quad + b(m^2 - n^2 + 4b^2)A_{22}^{(3)} - 2bmnA_{11}^{(4)} + n(m^2 + n^2 - 4b^2)A_{12}^{(4)} + 2bmnA_{22}^{(4)}] \\ &\quad + 2(A_{24}^{(1)} + A_{14}^{(2)})(m^2 + n^2)[n(4b^2 - m^2 - n^2)A_{12}^{(3)} + m(m^2 + n^2 + 4b^2)A_{12}^{(4)} \\ &\quad - b(m^2 - n^2 + 4b^2)A_{11}^{(4)} - 2bmnA_{22}^{(3)} + b(m^2 - n^2 + 4b^2)A_{22}^{(4)} + 2bmnA_{11}^{(3)}] \\ &\quad + (3A_{13}^{(1)} + A_{23}^{(2)})[m(m^2 + n^2)^2A_{11}^{(3)} + 2b^2m(4b^2 + 3m^2 - n^2)A_{11}^{(3)} \\ &\quad + 2b(m^2 + n^2)(m^2 - n^2 + 4b^2)A_{12}^{(3)} - 2b^2m(3n^2 - m^2 - 4b^2)A_{22}^{(3)} + n(m^2 + n^2)^2A_{11}^{(4)} \\ &\quad + 2b^2n(m^2 - 3n^2 + 4b^2)A_{11}^{(4)} + 4mnb(m^2 + n^2)A_{12}^{(4)} + 2b^2n(4b^2 + 3m^2 - n^2)A_{22}^{(4)}] \\ &\quad + (3A_{14}^{(1)} + A_{24}^{(2)})[2b^2n(3n^2 - m^2 - 4b^2)A_{11}^{(3)} - n(m^2 + n^2)^2A_{11}^{(3)} \\ &\quad - 4mnb(m^2 + n^2)A_{12}^{(3)} - 2b^2n(3m^2 + 4b^2 - n^2)A_{22}^{(3)} + m(m^2 + n^2)(m^2 + n^2 + 6b^2)A_{11}^{(4)} \\ &\quad + 8mb^2(b^2 - n^2)A_{11}^{(4)} - 2b(m^2 + n^2)(n^2 - m^2 - 4b^2)A_{12}^{(4)} + 2b^2m(m^2 - 3n^2 + 4b^2)A_{22}^{(4)}] \\ &\quad + (3A_{23}^{(2)} + A_{13}^{(1)})[2b^2m(4b^2 + m^2 - 3n^2)A_{11}^{(3)} - 2b(m^2 + n^2)(m^2 - n^2 + 4b^2)A_{12}^{(3)} \\ &\quad - 2b^2m(n^2 - 4b^2 - 3m^2)A_{22}^{(3)} + m(m^2 + n^2)^2A_{22}^{(3)} + 2b^2n(4b^2 + 3m^2 - n^2)A_{11}^{(4)} \\ &\quad - 4bmn(m^2 + n^2)A_{12}^{(4)} - 2nb^2(3n^2 - m^2 - 4b^2)A_{22}^{(4)} + n(m^2 + n^2)^2A_{22}^{(4)}] \\ &\quad + (3A_{24}^{(2)} + A_{14}^{(1)})[4bmn(m^2 + n^2)A_{12}^{(3)} - 2b^2n(3m^2 + 4b^2 - n^2)A_{11}^{(3)} - n(m^2 + n^2)^2A_{22}^{(3)} \\ &\quad - 2b^2n(m^2 - 3n^2 + 4b^2)A_{22}^{(3)} + 2b^2m(4b^2 + m^2 - 3n^2)A_{11}^{(4)} \\ &\quad - 2b(m^2 + n^2)(4b^2 + m^2 - n^2)A_{12}^{(4)} + m(m^2 + n^2)^2A_{22}^{(4)} + 2b^2m(3m^2 + 4b^2 - n^2)A_{22}^{(4)}]. \end{aligned}$$

Here

$$L_{1,\text{cub}} = \frac{\cos^9(\alpha)(1 - 19 \cos(2\theta_0))}{32p \cos^8(\theta_0)(\cos^2(\alpha) + 4p^2 \cos^4(\theta_0))} \tag{26}$$

denotes the contributions by the cubic terms in (23), the entry

$$L_{1,\text{nf}} = \frac{\cos^9(\alpha) (\cos^2(\alpha) \sin^2(\theta_0) - 3p^2 \cos^6(\theta_0))}{p \cos^8(\theta_0) (\cos^2(\alpha) + 4p^2 \cos^4(\theta_0))^2} \tag{27}$$

is obtained by eliminating the quadratic terms in  $(\xi_1, \xi_2)$  in  $Q_1$  and  $Q_2$  in (24) by Normal Form, and

$$\frac{2b}{\Delta} L_{1,\text{cm}} = \frac{-\cos^9(\alpha) (9 \cos^2(\alpha) - 8p^2 \cos^2(\theta_0) + 38p^2 \cos^4(\theta_0))}{2p \cos^6(\theta_0) (\cos^2(\alpha) + 4p^2 \cos^4(\theta_0))^2} \tag{28}$$

denotes the contributions by projecting the equations onto the center manifold.

Summing the three expressions (26), (27) and (28) yields the astonishingly simple result (14).

## References

1. Pars, L.: *A Treatise on Analytical Dynamics*. Heinemann, London (1965)
2. Routh, E.J.: *Dynamics of a System of Rigid Bodies*. Dover Publications, New York (1955)
3. Sinopoli, A.: Unilaterality and dry friction: a geometric formulation for two-dimensional rigid body dynamics. *Nonlinear Dyn.* **12**(4), 343–366 (1997)
4. Karapetyan, A.V.: The movement of a disc on a rotating horizontal plane with dry friction. *J. Appl. Math. Mech.* **80**(5), 376–380 (2016)
5. Ehrlich, R., Tuszynski, J.: Ball on a rotating turntable: comparison of theory and experiment. *Am. J. Phys.* **63**, 351 (1995)
6. Udwardia, F.E., Di Massa, G.: Sphere rolling on a moving surface: application of the fundamental equation of constrained motion. *Simul. Model. Pract. Theory* **19**(4), 1118–1138 (2011)
7. Fleissner, F., Lehnart, A., Eberhard, P.: Dynamic simulation of sloshing fluid and granular cargo in transport vehicles. *Veh. Syst. Dyn.* **48**(1), 3–15 (2010)
8. Alkhalidi, H., Ergenzinger, C., Fleissner, F., Eberhard, P.: Comparison between two different mesh descriptions used for simulation of sieving processes. *Granul. Matter* **10**(3), 223–229 (2008)
9. Brouwer, L.E.J.: *Collected Works*, vol. II. North-Holland, Amsterdam (1976)
10. Akshat, A., Sahil, G., Toby, J.: Particle sliding on a turntable in the presence of friction. *Am. J. Phys.* **83**, 126–132 (2015)
11. Burov, A.A.: On bifurcations of relative equilibria of a heavy bead sliding with dry friction on a rotating circle. *Acta Mech.* **212**(3), 349–354 (2010)
12. Burov, A.A., Yakushev, I.A.: Bifurcations of relative equilibria of a heavy bead on a rotating hoop with dry friction. *J. Appl. Math. Mech.* **78**(5), 460–467 (2014)
13. Bautin, N.N.: *Behaviour of Dynamical Systems Near the Boundaries of the Stability Region*. Gostekhizdat, Moscow (1949)
14. Lyapunov, A.: *General Problem of the Stability of Motions*. CRC Press, Moscow (1992)
15. Shalimova, E.S.: Steady and periodic modes in the problem of motion of a heavy material point on a rotating sphere (the viscous friction case). *Moscow Univ. Mech. Bull.* **69**, 89–96 (2014)
16. Kuznetsov, Y.A.: *Elements of Applied Bifurcation Theory*. Springer, New York (1995)
17. Wiggins, S.: *Introduction to Applied Nonlinear Dynamical Systems and Chaos*, 2nd edn. Springer, New York (2003)
18. Oberle, H.J., Grimm, W., Berger, E.: BNDSCO, Rechenprogramm zur Lösung beschränkter optimaler Steuerungsprobleme. Techn. Univ. München (1985)
19. Seydel, R.: A continuation algorithm with step control. In: *Numerical Methods for Bifurcation Problems*. ISNM 70. Birkhäuser (1984)

**Publisher's Note** Springer Nature remains neutral with regard to jurisdictional claims in published maps and institutional affiliations.